Near-Infrared Coronagraphic Observations of a Classical TTauri Star, DO Taurus

Itoh, Yoichi ; Hayashi, Masahiko ; Tamura, Motohide ; Oasa, Yumiko ; Hioki, Tomonori ; Fukagawa, Misato ; Kudo, Tomoyuki

(Citation)
Publications of the Astronomical Society of Japan,60(2):223-226

(Issue Date)
2008-04-25

(Resource Type)
journal article

(Version)
Version of Record

PASJ: Publ. Astron. Soc. Japan **60**, 223–226, 2008 April 25

Near-Infrared Coronagraphic Observations of a Classical T Tauri Star, DO Taurus*

Yoichi ITOH,[1] Masahiko HAYASHI,[2] Motohide TAMURA,[3] Yumiko OASA,[1] Tomonori HIOKI,[1]
Misato FUKAGAWA,[4] and Tomoyuki KUDO[5]
[1]*Graduate School of Science, Kobe University, 1-1 Rokkodai, Nada-ku, Kobe 657-8501*
yitoh@kobe-u.ac.jp
[2]*Subaru Telescope, National Astronomical Observatory of Japan, 650 North A'ohoku Place, Hilo, HI 96720, USA*
[3]*National Astronomical Observatory, 2-21-1 Osawa, Mitaka, Tokyo 181-8588*
[4]*Graduate School of Science, Nagoya University, Furo-cho, Chikusa-ku, Nagoya 464-8601*
[5]*Graduate University for Advanced Studies, 2-21-1 Osawa, Mitaka, Tokyo 181-8588*

(Received 2007 April 26; accepted 2007 November 8)

Abstract

A high angular resolution near-infrared image of a classical T Tauri star, DO Tau, was obtained with Coronagraphic Imager with Adaptive Optics (CIAO) mounted on the Subaru Telescope. Circumstellar emission was detected at $\sim 1\farcs7$ from the central star in the direction of the redshifted jet. No emission was found toward the opposite direction. We also found one faint point source $3\farcs46$ away from the central star. The following observation will reveal whether it is an associated planetary mass object or a background object.

Key words: stars: individual (DO Taurus) — stars: pre-main sequence — techniques: high angular resolution

1. Introduction

Circumstellar disks around T Tauri stars have a variety of forms, structures, and physical characteristics, which are considered to be the origin of the diversity of planetary systems. High spatial resolution images of circumstellar disks have been obtained in optical and near-infrared wavelengths, using ground-based large-aperture telescopes equipped with adaptive optics systems (AO), or the Hubble Space Telescope (HST). Spatial resolutions obtained with such telescopes are as high as $0\farcs1$, corresponding to 15 AU at a distance of nearby star-forming regions. For example, the circumbinary disk around the GG Tau A system is clearly detected using adaptive optics systems with ground-based telescopes (Roddier et al. 1996; Itoh et al. 2002) and HST (Silber et al. 2000; McCabe et al. 2002; Krist et al. 2002, 2005). However, most of the circumstellar disks detected so far are disks around binaries (e.g., GG Tau, UY Aur: Hioki et al. 2007), edge-on disks (e.g., HH 30: Ray et al. 1996), disks around massive young stellar objects (YSOs) (e.g., AB Aur: Fukagawa et al. 2004), and disks around active YSOs (e.g., HL Tau: Lucas et al. 2004).

We present here a high-resolution near-infrared coronagraphic image of DO Tau. This star is a classical T Tauri star associated with the Taurus molecular cloud. The mass, age, and visual extinction of the star are estimated to be $\sim 0.3 M_\odot$, $\sim 2 \times 10^5$ yr, and 4.6 mag, respectively (Hartigan et al. 1995). While L-band speckle observations suggest a faint companion (~ 9 mag) with a separation of $0\farcs19$ at the position angle (PA) of 300°(Tessier et al. 1994), K-band speckle observations did not detect any companions (Ghez et al. 1993; Leinert et al. 1993; White & Ghez 2001). DO Tau has a reflection nebula extending northeastward, which is classified as a cometary nebula (Magakian 2003). A circumstellar disk was discovered by radio observations, whose mass is estimated to be $0.01 \pm 0.005\ M_\odot$ (Koerner et al. 1995) or $0.004\ M_\odot$ (Kitamura et al. 2002). The PA of the major axis of the disk was derived to be 160° (Koerner & Sargent 1995), while it is suggested to be 67° by Kitamura et al. (2002). Optical dipole jets emanate from the central star with a PA of 70° for the redshifted jet and 250° for the blueshifted one (Hirth et al. 1994). Since it is generally considered that the major axis of a circumstellar disk is perpendicular to the PA of a bipolar jet, we use 160° for the PA of the major axis of the disk. Both infrared and optical polarizations have a position angle of $\sim$175° (Bastien et al. 1982; Tamura & Sato 1989). This angle is consistent with the PA of the major axis of the disk if scattering occurs in the near or far side of the disk plane, perpendicular to the optical jets. With these characteristics of the star and its associations, DO Tau displays most of the known properties of classical T Tauri stars.

2. Observations and Data Reduction

Near-infrared coronagraphic observations were carried out on 2005 November 11 with Coronagraphic Imager with Adaptive Optics (CIAO) mounted on the Subaru Telescope. CIAO has occulting masks at the first focal plane and Lyot stops at the pupil plane. The mask that we used was $0\farcs8$ in diameter. The occulting masks are made of chromium on a glass substrate, and have a transmittance of a few tenths of a percent, which enables us to measure the exact position of a bright central object. We used the traditional circular Lyot stop, whose diameter was 0.8 times as large as the pupil diameter. The 1024×1024 InSb Alladin II array detector was located at the second focal plane. The field of view is $21\farcs8 \times 21\farcs8$ with a spatial scale of $0\farcs02133$ pixel^{-1}. The uncertainty in the pixel scale was $0\farcs00003$ pixel^{-1} and that in the position angle was $0\fdg07$. The observations were carried out in the

* Based on data collected at the Subaru Telescope, which is operated by the National Astronomical Observatory of Japan.

H-band, while wavefront sensing was performed in the optical wavelengths. As a PSF reference star, we observed SAO 57537 immediately before and after observations of DO Tau with the same configurations. Using a neutral-density filter in the AO system, we reduced the optical intensity of the PSF reference star, in order to match the PSF of DO Tau with that of the PSF reference star. As a result, the optical intensities into the wavefront sensor ranged from 38800 to 41700 counts for DO Tau and from 35200 to 39700 counts for the PSF reference star, respectively. The typical seeing size was 0.″9. Using the AO, the FWHM of the PSF was improved to be as good as 0.″11. For DO Tau, the exposure time was 6 s, and we coadded 2 exposures into one frame. After we took 50 frames, the telescope pointing and the occulting mask were dithered by about 1″; we then took another 50 frames. The star was centered on the mask for all frames. For the PSF reference star, we took 60 and 30 frames immediately before and after the observations of DO Tau, respectively. Each frame consists of a single image of 10 s exposure. We also took FS 125 (Hawarden et al. 2001) as a photometric standard. Sky flats were taken at the beginning of the night, and dark frames at the end.

The Image Reduction and Analysis Facility (IRAF) software was used for all data reduction. First, a dark frame was subtracted from each of the object frames, and then the frames were divided by the sky-flat. Hot and bad pixels were removed. The peak position of the PSF changed slightly during the observations. This was due to differences in the atmospheric distortion between the infrared wavelengths at which the images were taken and the optical wavelengths at which the wavefront was sensed. After we measured the peak position of the reference star PSF with the RADPROFILE task, the images were shifted. Since the Subaru Telescope is of the altazimuth type and we used the instrument rotator, the PA of the spider changed with time. The frames of the reference star were rotated so as to adjust the PA of the spider to match that of each object frame, and were then combined. Next, we measured the peak position of DO Tau with the RADPROFILE task in each frame. The combined reference image was shifted so as to adjust the peak position of the PSFs between the reference star and DO Tau.

When deciding the factor to multiply the reference PSF so that it would match in intensity of the target PSF, the region 0.″5–1.″3 was used. Within 0.″5, the PSF varied too much due to the AO system, and outside 1.″3 there was not a sufficient signal to derive a reliable factor. The reference image was renormalized to match the wing emission of the DO Tau image in this annulus. Finally, the scaled reference image was subtracted from the object frame. Any mismatch of the PSFs between the object and the reference made false residuals in the PSF subtracted image. We inspected the PSF subtracted images by eye, and judged that the halo component was successfully subtracted in 83 frames. We combined these 83 object frames into one frame. The effective total integration time for the object was 996 s.

DO Tau was also observed by the Space Telescope Imaging Spectrograph (STIS) on the Hubble Space Telescope in 2001 December and 2003 February (PI: C. Grady). The observations were carried out in the coronagraphic imaging mode without any broad-band filter. The exposure time was 2268 s, and two frames were taken. The second frame was obtained with a 30°offset in the PA to the first frame.

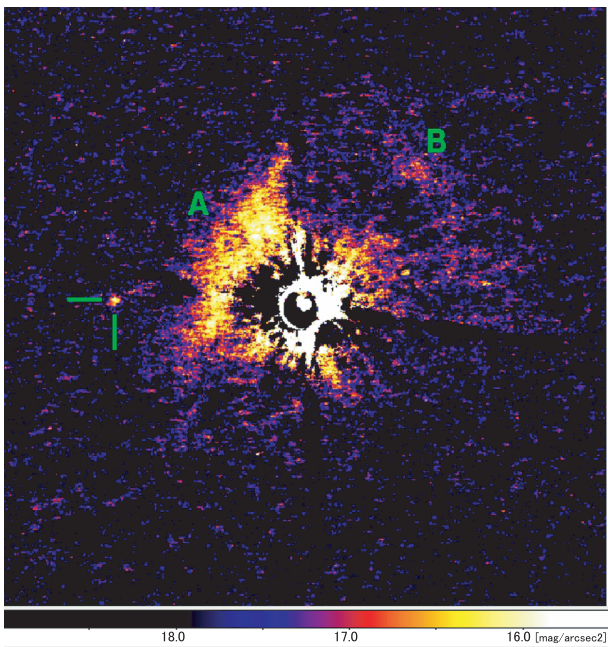

Fig. 1. H-band coronagraphic image of DO Tau. The field of view is 11.″0 × 11.″0. North is up, and east is to the left. The central star blocked by the mask is located at the center of the image. Its PSF was subtracted. A circumstellar emission was detected at ∼ 1.″7 northeast of the star (labeled "A"). Another structure was marginally detected 3.″2 northwest of the star (labeled "B"). A negative cross was artificially created from the diffraction pattern of the spiders. One point source was detected 3.″46 east of the central star, marked by lines.

We used HR 957 images (PI: C. Grady) as the PSF reference, and then the PSF of DO Tau was subtracted in each frame. Counts were replaced by zero in the region where the diffraction pattern of the spider dominated. Next, the second frame was rotated by −30°, so that the PAs of both frames were adjusted. We then took average counts for the two frames, except for the regions blocked by the coronagraph mask, or replaced by zero counts in one of the two frames. In such regions, the counts of another frame were used.

3. Results and Discussion

3.1. The Nebula

An H-band coronagraphic image of DO Tau is presented in figure 1. The star within the occulting mask is located at the center of the image. The halo of the star is significantly suppressed by subtracting the image of the PSF reference star. The bright portions just around the star are artifacts made by residuals in the halo of the star. Noteworthy is a circumstellar emission 1.″7 away from the central star with PA ∼45° (the region A in figure 1). Another structure is marginally detected 3.″2 away from the star with PA ∼ 320° (labeled "B").

The northeast emission structure is elongated. Its size is 1.″2 × 4.″0 (170 AU × 560 AU). An inner boundary of the structure is around 1.″1 (150 AU) from the central star. The surface

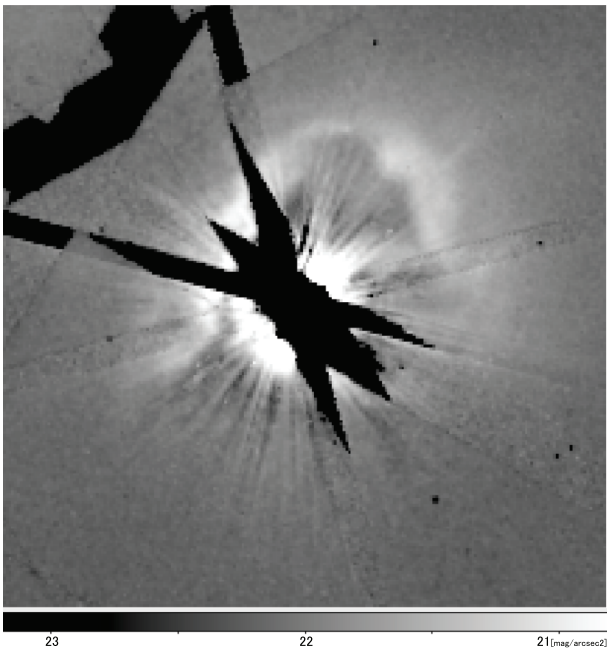

Fig. 2. Optical image of DO Tau taken by STIS on the Hubble Space Telescope. The field of view is $11\farcs0 \times 11\farcs0$. North is up, and east is to the left. The PSF of the central star was subtracted. The regions obscured by the coronagraphic wedges or diffraction of the spider are blacked out. Both nebulae in the northeast and northwest of the star were detected.

brightness of the structure was calculated to be 16.6 mag arcsec^{-2}, which is 3 mag fainter than that of the faintest portion of the circumbinary disk around GG Tau (Itoh et al. 2002). The structure is located in the direction of the redshifted jet. It should be noted that two of the spiders may be obscuring a part of the emission. Since the PAs of the spiders changed from 3°to 8°and 79°to 84°during the integration, the detected emission of the structure may be limited. This circumstellar structure is asymmetric with respect to the star. We examined the detection limit for a circumstellar structure by adding an image of the northeast structure to the opposite side of the star. The structure in the southwest direction could be detected with $\sim 1\,\sigma$, if the brightness ratio (brightness of the northeast structure compared with that of the southwest one) is smaller than 5.

The northwest nebula is very faint. Its size is about $3\farcs4 \times 4\farcs7$ (480 AU × 660 AU). The surface brightness of the nebula is about 18 mag arcsec^{-2}.

Figure 2 shows the optical image of DO Tau. In the figure, both the northeast emission and the northwest nebula are revealed, as are seen in the near-infrared image. The optical image indicates that the northwest and northeast nebulae are joined and are part of the same structure. We propose that it is a cleared cavity. Since the bright northeast nebula is located in the direction of the redshifted jet, we expect that it is located near to us. Forward scattering from dust grains in the nebula reasonably explains the northeast/southwest brightness asymmetry. However, any simple geometric model cannot account for the northwest/southeast asymmetry, even if anisotropic scattering is considered. We did not find significant difference in color between the northeast emission and the northwest nebula. We noticed that DO Tau increased its flux by about 0.7 magnitude in the two STIS observational epochs.

3.2. The Point Source

We found no evidence for a close companion, as suggested by Tessier, Bouvier, and Lacombe (1994). Instead, we found one faint point source (DO Tau B) located $3\farcs46$ away from the central star. It has 20.4 mag at the H-band.

On the other hand, it was not detected in the HST optical image. We estimated the detection limit for a point source by adding pseudo-PSF to the processed data. We placed Gaussian PSFs with a FWHM of $0\farcs12$ (2.4 pixels) at the same position of the near-infrared point source. A point source with $2.5 \times 10^{-19}\,\mathrm{W\,m^{-2}}\mu\mathrm{m}^{-1}$ could be detected, while that with $1.6 \times 10^{-19}\,\mathrm{W\,m^{-2}}\mu\mathrm{m}^{-1}$ could not. These correspond to 27.8 mag and 28.3 mag at the V-band, respectively, though accurate magnitudes cannot be estimated due to the observation with a clear aperture. We conclude that the detection limit for the point source is about 28 mag in the optical image.

The point source may be a faint companion of DO Tau. The age of DO Tau is estimated to be 2×10^5 yr (Hartigan et al. 1995). Based on the evolutionary track of Baraffe et al. (1998), a 1 M_J object with $A_V \sim 5$ mag in the Taurus molecular cloud has $H \sim 21$ mag at 1 Myr. Such an object would have 36 mag at the V-band, consistent with negative detection of the point source in the optical image.

Otherwise, the object may be a background star. Based on a star-count model of the Galaxy (Jones et al. 1981), 0.05 background objects are expected in a $3\farcs46$ radius circle toward the Taurus molecular cloud with a limiting magnitude of 21 at the H-band and $A_V \sim 5$ mag. An A0 background star with $A_V = 5$ mag would have 26 mag in the V-band. This is inconsistent with negative detection of the source in the optical image. If it is a K- or M-type background star, its V-band magnitude is fainter than the limiting magnitude in the optical image. Following spectroscopy and astrometry will confirm its companionship.

4. Conclusion

We carried out near-infrared coronagraphic observations of a classical T Tauri star DO Tau. An asymmetric emission around DO Tau was detected at $\sim 1\farcs7$ northeast of the central star. We did not detect any emission in the opposite direction. This emission structure is interpreted as being a cleared cavity with anisotropic scattering. We also found one faint point source $3\farcs46$ away from DO Tau. Its H-band magnitude is 20.4 mag, suggesting 1 M_J if the point source is associated with DO Tau.

This work is supported by "The 21st Century COE program: The Origin and Evolution of Planetary Systems" of the Ministry of Education, Culture, Sports, Science and Technology (MEXT). Y. I. is supported by a Grant-in-Aid for Scientific Research (No. 16740256).

References

Baraffe, I., Chabrier, G., Allard, F., & Hauschild, P. H. 1998, A&A, 337, 403
Bastien, P. 1982, A&AS, 48, 153
Fukagawa, M., et al. 2004, ApJ, 605, L53
Ghez, A. M., Neugebauer, G., & Matthews, K. 1993, AJ, 106, 2005
Hartigan, P., Edwards, S., & Ghandour, L. 1995, ApJ, 452, 736
Hawarden, T. G., Leggett, S. K., Letawsky, M. B., Ballantyne, D. R., & Casali, M. M. 2001, MNRAS, 325, 563
Hioki, T., et al. 2007, AJ, 134, 880
Hirth, G. A., Mundt, R., Solf, J., & Ray, T. P. 1994, ApJ, 427, L99
Itoh, Y., et al. 2002, PASJ, 54, 963
Jones, T. J., Ashley, A., Hyland, A. R., & Ruelas-Mayorga, A. 1981, MNRAS, 197, 413
Kitamura, Y., Momose, M., Yokogawa, S., Kawabe, R., Tamura, M., & Ida, S. 2002, ApJ, 581, 357
Koerner, D. W., Chandler, C. J., & Sargent, A. I. 1995, ApJ, 452, L69
Koerner, D. W., & Sargent, A. I. 1995, AJ, 109, 2138
Krist, J. E., et al. 2005, AJ, 130, 2778
Krist, J. E., Stapelfeldt, K. R., & Watson, A. M. 2002, ApJ, 570, 785
Leinert, Ch., Zinnecker, H., Weitzel, N., Christou, J., Ridgway, S. T., Jameson, R., Haas, M., & Lenzen, R. 1993, A&A, 278, 129
Lucas, P. W., et al. 2004, MNRAS, 352, 1347
Magakian, T. Y. 2003, A&A, 399, 141
McCabe, C., Duchêne, G., & Ghez, A. M. 2002, ApJ, 575, 974
Ray, T. P., Mundt, R., Dyson, J. E., Falle, S. A. E. G., & Raga, A. C. 1996, ApJ, 468, L103
Roddier, C., Roddier, F., Northcott, M. J., Graves, J. E., & Jim, K. 1996, ApJ, 463, 326
Silber, J., Gledhill, T., Duchêne, G., & Ménard, F. 2000, ApJ, 536, L89
Tamura, M., & Sato, S. 1989, AJ, 98, 1368
Tessier, E., Bouvier, J., & Lacombe, F. 1994, A&A, 283, 827
White, R. J., & Ghez, A. M. 2001, ApJ, 556, 265